

Induction of Siglec-G by RNA Viruses Inhibits the Innate Immune Response by Promoting RIG-I Degradation

Weilin Chen,^{1,4} Chaofeng Han,^{2,4} Bin Xie,^{1,4} Xiang Hu,³ Qian Yu,² Liyun Shi,¹ Qingqing Wang,¹ Dongling Li,³ Jianli Wang,¹ Pan Zheng,³ Yang Liu,³ and Xuetao Cao^{1,2,3,*}

¹Institute of Immunology, Zhejiang University School of Medicine, Hangzhou 310058, China

²National Key Laboratory of Medical Immunology and Institute of Immunology, Second Military Medical University, Shanghai 200433, China

³National Key Laboratory of Medical Molecular Biology and Department of Immunology, Chinese Academy of Medical Sciences, Beijing 100005, China

⁴These authors contributed equally to this work

*Correspondence: caoxt@immunol.org

<http://dx.doi.org/10.1016/j.cell.2013.01.011>

SUMMARY

RIG-I is a critical RNA virus sensor that serves to initiate antiviral innate immunity. However, post-translational regulation of RIG-I signaling remains to be fully understood. We report here that RNA viruses, but not DNA viruses or bacteria, specifically upregulate lectin family member *Siglecg* expression in macrophages by RIG-I- or NF- κ B-dependent mechanisms. Siglec-G-induced recruitment of SHP2 and the E3 ubiquitin ligase c-Cbl to RIG-I leads to RIG-I degradation via K48-linked ubiquitination at Lys813 by c-Cbl. By increasing type I interferon production, targeted inactivation of *Siglecg* protects mice against lethal RNA virus infection. Taken together, our data reveal a negative feedback loop of RIG-I signaling and identify a Siglec-G-mediated immune evasion pathway exploited by RNA viruses with implication in antiviral applications. These findings also provide insights into the functions and crosstalk of Siglec-G, a known adaptive response regulator, in innate immunity.

INTRODUCTION

Innate immunity is the first line of host defense against virus infection. Pattern recognition receptors (PRRs), including Toll-like receptors (TLRs) and RIG-I-like receptors (RLRs), are main sensors of the invading viruses (Kawai and Akira, 2010; Barbalat et al., 2011; Rehwinkel and Reis e Sousa, 2010). TLR3, 7, 8, and 9 detect viral RNAs and DNAs in the endosome, whereas RLR members RIG-I and MDA5 sense viral RNAs in the cytoplasm (Kato et al., 2011). Upon recognizing invading viruses, PRRs activate downstream signaling pathways to initiate innate immune response through the induction of type I interferons (IFNs). TLRs-mediated signaling pathways recruit adaptor proteins such as MyD88 and TIR-domain-containing adaptor-inducing

IFN- β (TRIF), leading to the activation of transcription factors that regulate the expression of proinflammatory cytokines and type I IFNs (Kawai and Akira, 2011). RIG-I and MDA5 both contain DExD/H box RNA helicase with two caspase-recruiting domain (CARD)-like sequences and a helicase domain (Yoneyama et al., 2004; 2005). RIG-I, the most important member of RLHs, recognizes cytoplasmic viral RNA such as that of hepatitis V virus and influenza virus and induces IFN- β production (Kowalinski et al., 2011; Seth et al., 2005; Hou et al., 2011; O'Neill and Bowie, 2011). Insufficient IFN production causes chronic infection, whereas excessive IFN causes autoimmune and/or inflammatory diseases. Thus, precise control of RIG-I signaling is critical for efficient viral clearance without harmful immunopathology.

The different kinds of PRRs can cross-regulate their downstream signaling events in either a synergistic or antagonistic manner (Kawai and Akira, 2011). Extensive interplays between PRRs and other pivotal immune mediators and receptors also orchestrate the outcome of host innate immune defenses. For example, the activation of RLR resulted in the selective suppression of transcription of the gene encoding the p40 subunit of interleukin 12 that was effectively induced by the activation of TLRs. Cross-interference of RLR and TLR signaling pathways modulates antibacterial T cell responses (Negishi et al., 2012). The distinct classes of PRRs overlap in the spectrum of pathogen-associated molecular patterns (PAMPs) that they recognized and cross-integrate their downstream signal pathways; PRRs signaling is also cross-modulated by signaling generated via other membrane-associated receptors. For example, innate immunity utilizes members of the host lectin family (i.e., C-type lectin receptors, sialic-acid-binding immunoglobulin-like lectins [Siglecs], and galectins) as PRRs to detect viruses or transduce signals (van Kooyk and Rabinovich, 2008; Vasta, 2009). However, the role of lectins in innate immune response and their crosstalk with the RIG-I pathway in antiviral innate response have not been established.

Our systemic analyses identified several genes of lectin family that were upregulated significantly in macrophages in response to infection with RNA viruses. Among them, we focused on

Siglec-G, as it was upregulated the most and the quickest upon RNA virus infection. Moreover, our experiments indicated that knocking down *Siglecg* with siRNA in macrophages increased the VSV-induced IFN- β mRNA expression most potently compared with knocking down other lectin genes. These preliminary results indicated the importance of Siglec-G in antiviral innate immunity. In addition, the mouse homolog of human Siglec-10 had been independently identified by us and others (Li et al., 2001; Munday et al., 2001; Whitney et al., 2001), and the functional study of Siglec-G attracted our attention. Siglec-G belongs to the family of Siglecs, which has intracellular domains with ITIM (Pillai et al., 2012), known as inhibitory receptor of B1 cells (Hoffmann et al., 2007; Ding et al., 2007). Recent studies demonstrate that the CD24-Siglec-G/10 interaction is important for the negative regulation of host response to danger-associated molecular patterns (DAMPs) (Chen et al., 2009, 2011). However, the biological functions of Siglec-G and its role in antiviral innate immunity remained elusive.

Ubiquitination is one of the most versatile posttranslational modifications and is also indispensable for antiviral infection. Posttranslational modification of RIG-I and downstream signaling proteins by different types of ubiquitination has been found to be a key event in the regulation of RIG-I-triggered NF- κ B and IRF3 activation (Loo and Gale, 2011). K63-linked ubiquitination by TRIM25 (Gack et al., 2007), or RING finger protein leading to RIG-I activation (Riplet/REUL/RNF135) (Oshiumi et al., 2009) and free K63-linked polyubiquitin chains (Zeng et al., 2010) have been shown to induce RIG-I activation. On the other hand, RIG-I also undergoes ubiquitination by RNF125 for proteasomal degradation (Arimoto et al., 2007). However, which and how ubiquitin ligases and ubiquitin binding scaffold proteins contribute to regulation of RIG-I signaling remains to be illuminated.

Here, we report that RNA virus infection upregulates *Siglecg* expression via the NF- κ B pathway. Mice with targeted mutation of *Siglecg* are protected against vesicular stomatitis virus (VSV) infection with much more type I IFN production. Siglec-G associates with c-Cbl and RIG-I via SHP2, promoting RIG-I proteasomal degradation after conjugation to K48-linked ubiquitin by c-Cbl. Our data demonstrate a negative feedback regulation of RIG-I-mediated antiviral innate immune response through posttranslational modification of RIG-I.

RESULTS

RNA Viral Infection Specifically Upregulates *Siglecg* Expression in Macrophages via NF- κ B-Dependent Mechanism

In order to identify molecules selectively involved in the regulation of innate response against RNA viral infection, we analyzed gene expression profiles in mouse peritoneal macrophages infected with the RNA virus VSV. Focusing on the expression of lectin family genes, we found that VSV infection significantly changed the mRNA level of several lectins, including C-type lectin receptors and Siglecs (Figure 1A). Upregulation of the expression of a panel of lectin family genes was further validated by quantitative PCR (Q-PCR) in macrophages infected with various pathogens, including VSV, DNA virus (herpes simplex

virus I [HSV-1]), intracellular bacteria (*Listeria monocytogenes* [LM]), or extracellular Gram-negative bacteria (*Escherichia coli* [*E. coli*]). Among these genes, the mRNA level of Siglec-G was upregulated most significantly and quickly from 4 to 12 hr after infection with VSV, but not by infection with HSV-1, LM, or *E. coli* (Figure 1B). siRNA knockdown of *Siglecg* in macrophages increased the VSV-induced IFN- β mRNA expression most potently compared with knocking down other lectin genes (Figure S1A available online). Upregulation of *Siglecg* expression was VSV (MOI) dose dependent (Figure S1B). Further, *Siglecg* was upregulated in macrophages transfected with poly(I:C) or infected with another RNA virus, the Sendai virus (SeV), but remained unchanged in macrophages stimulated with various TLR ligands or transfected with LM genomic DNA, poly(dA:dT), or poly(dG:dC) (Figures 1C, S1C, and S1D). These data suggest that the infection of RNA viruses, but not DNA viruses or bacteria, specifically upregulates *Siglecg* expression in macrophages.

We further assessed VSV infection-induced *Siglecg* expression in peritoneal macrophages derived from *Rigi*^{-/-}, *Irf3*^{-/-}, *Ifn β* ^{-/-}, or *Ifn α β R*^{-/-} mice and wild-type (WT) mice-derived peritoneal macrophages pretreated with PDTC, a NF- κ B inhibitor, PD98059 (MEK inhibitor), SP600125 (JNK inhibitor), SB203580 (P38 inhibitor), Wortmannin (PI3K inhibitor), or Gö 6976 (PKC inhibitor). VSV-infection-induced upregulation of *Siglecg* expression was attenuated in *Rigi*^{-/-} macrophages or WT macrophages pretreated with PDTC (Figures 1D, 1E, and S1E). VSV-infection-induced upregulation of *Siglecg* expression was unaffected in *Irf3*^{-/-}, *Ifn β* ^{-/-}, or *Ifn α β R*^{-/-} mice-derived macrophages as compared to WT mice-derived macrophages (Figure S1F). Consistent with a role for NF- κ B, *Siglecg* promoter-luc activity increased in HEK293T cells ectopically overexpressing the p65 subunit of NF- κ B with or without RNA virus (SeV) infection (Figure S1G). The data suggest that RNA viral infection upregulates *Siglecg* expression via RIG-I-triggered NF- κ B signaling.

Histone modifications play important roles in the control of gene transcription. By ChIP assay, we found that H3K4me3 was upregulated and H3K27me3 was downregulated in the promoter of *Siglecg* gene in macrophages after VSV infection, whereas both H3K4me3 and H3K27me3 remained constant throughout the stimulation with LPS (Figure 1F). It has been reported that histone methyltransferase MLL mediates methylation of H3K4 (Wang et al., 2009), and another chromatin H3K4 methyltransferase, SET7/9, is an important coactivator of NF- κ B (Li et al., 2008). Chromatin immunoprecipitation (ChIP) experiments showed that VSV infection, but not LPS stimulation, could increase both SET7/9 and MLL enrichment at *Siglecg* promoter in macrophages (Figures 1G and 1H). Taken together, our findings demonstrate that RNA viral infection specifically upregulates *Siglecg* expression in macrophages via an NF- κ B-dependent mechanism and may also involve epigenetic modification of histone H3.

Siglecg Deficiency Protects Mice from Infection with RNA Viruses

To investigate the role and functional significance of Siglec-G in host antiviral innate response, we challenged *Siglecg*^{-/-} mice with RNA viruses VSV and SeV. VSV titer and replication

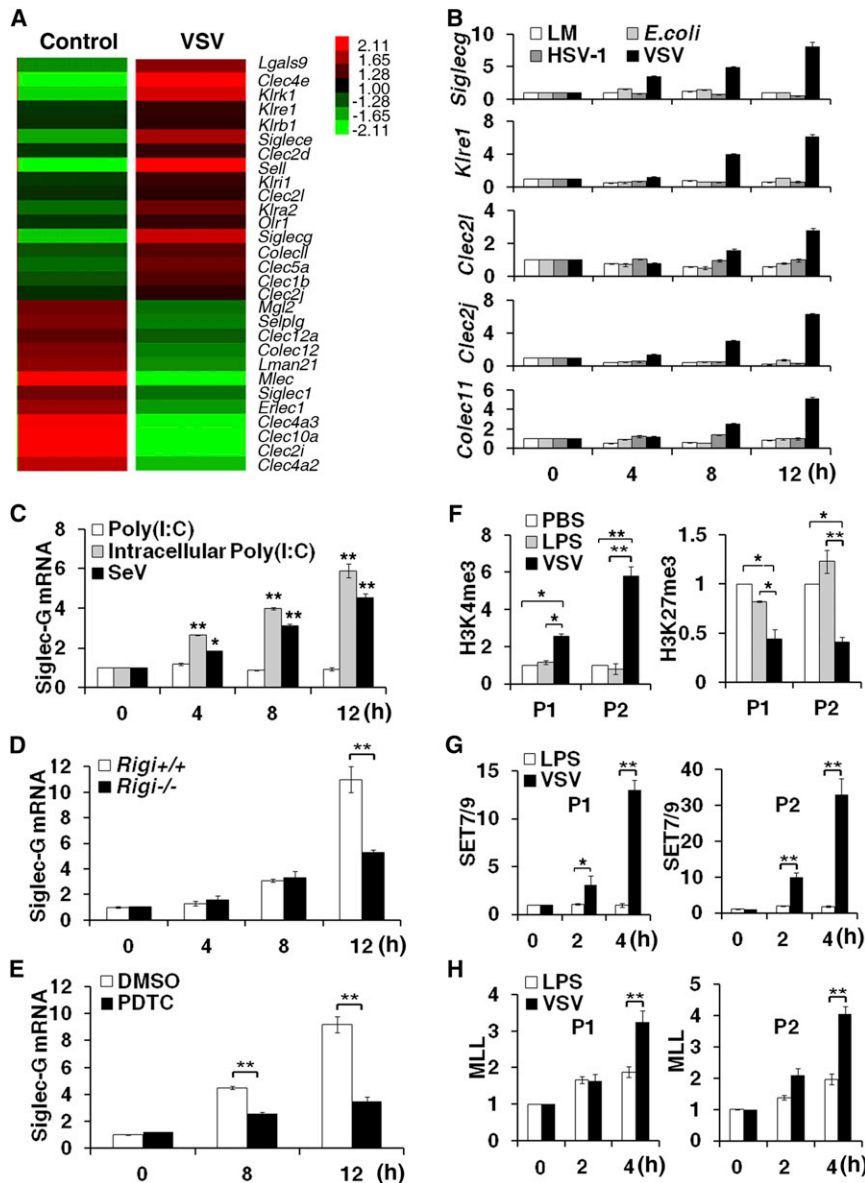


Figure 1. RNA Viral Infection Upregulates *Siglec-G* Expression by Histone H3 Modification through the NF- κ B Pathway

(A) Microarray analysis of mouse peritoneal macrophages infected with VSV. Shown is the heatmap of lectin family genes upregulated or downregulated in macrophages following VSV infection for 8 hr. Untreated macrophages were as control.

(B) Q-PCR analysis of *Siglec-G*, *Klr1*, *Clec2l*, *Clec2j*, and *Colecl1* mRNA expression in macrophages infected with LM, *E. coli*, HSV-1, or VSV for the indicated hours. Data were normalized to the expression of β -actin reference gene.

(C) Q-PCR analysis of *Siglec-G* mRNA expression in macrophages transfected with poly(I:C) (intracellular poly(I:C)), stimulated with poly(I:C), or infected with RNA virus SeV for the indicated hours.

(D) Q-PCR analysis of *Siglec-G* mRNA expression in *Rigi*^{-/-} macrophages infected with VSV.

(E) Q-PCR analysis of *Siglec-G* mRNA expression in macrophages pretreated for 1 hr with NF- κ B inhibitor PDTC (10 μ M) before VSV infection for indicated hours.

(F) ChIP analysis of macrophages treated for 4 hr with LPS or VSV by using H3K4me3 and H3K27me3 antibodies. Two sets of primers and probes (P1 and P2) of *Siglec-G* were used for Q-PCR.

(G and H) ChIP analysis of macrophages treated for indicated hours with LPS or VSV by using SET7/9 antibody (G) or MLL antibody (H).

Data are means \pm SEM. * p < 0.05; ** p < 0.01. See also Figure S1.

in organs from *Siglecg*^{-/-} mice were significantly reduced compared to *Siglecg*^{+/+} mice (Figures 2A and 2B). *Siglecg*^{-/-} mice were also more resistant to VSV infection in overall survival assays (Figure 2C). Less infiltration of inflammatory cells was observed in the lungs of *Siglecg*^{-/-} mice after infection with VSV (Figure 2D) or SeV (Figure S2A). Immunohistochemical staining for the macrophage glycoprotein F4/80 and neutrophil's azurophilic granules myeloperoxidase (MPO) demonstrated that less macrophages and neutrophils infiltrated in the lung from *Siglecg*^{-/-} mice than from *Siglecg*^{+/+} mice infected with VSV (Figure S2B). Similar infiltration of inflammatory cells was detected in the lungs from *Siglecg*^{-/-} and *Siglecg*^{+/+} mice infected with DNA virus HSV-1 (Figure S2A). Consistent with increased resistance, *Siglecg*^{-/-} mice produced higher levels of IFN- β than *Siglecg*^{+/+} mice in response to infection

with VSV (Figure 2E) or SeV (Figure S2C). In contrast, TNF- α and IL-6 production was unaffected by *Siglecg* deletion. We also noted higher IFN- β mRNA expression in the organs and peritoneal macrophages of *Siglecg*^{-/-} mice than in those of *Siglecg*^{+/+} mice infected with VSV (Figures 2F and 2G) or SeV (Figures S2D and S2E). Upregulation of IFN- β is also specific to RNA virus infection, as no significant difference in IFN- β production or mRNA expression was observed in mice infected with HSV-1 (Figures S2C–S2E). To further characterize the dynamics of chronic VSV infection, we measured VSV loads in lung homogenate supernatants and observed the pathological changes of lung from *Siglecg*^{-/-} and *Siglecg*^{+/+} mice infected with lower-dose VSV. As detected by TCID50 assay, VSV loads in organ samples from *Siglecg*^{-/-} mice were significantly lower than in organs from *Siglecg*^{+/+} mice on days 1 and 3, and VSV loads declined below the limitation of detection on day 5 and remained undetectable through day 14 postinfection (Figure S2F). Inflammatory changes observed in lungs were consistent with viral loads (Figure S2G). These data demonstrate that *Siglecg*^{-/-} mice develop more potent innate response against RNA viral infection by producing more IFN- β .

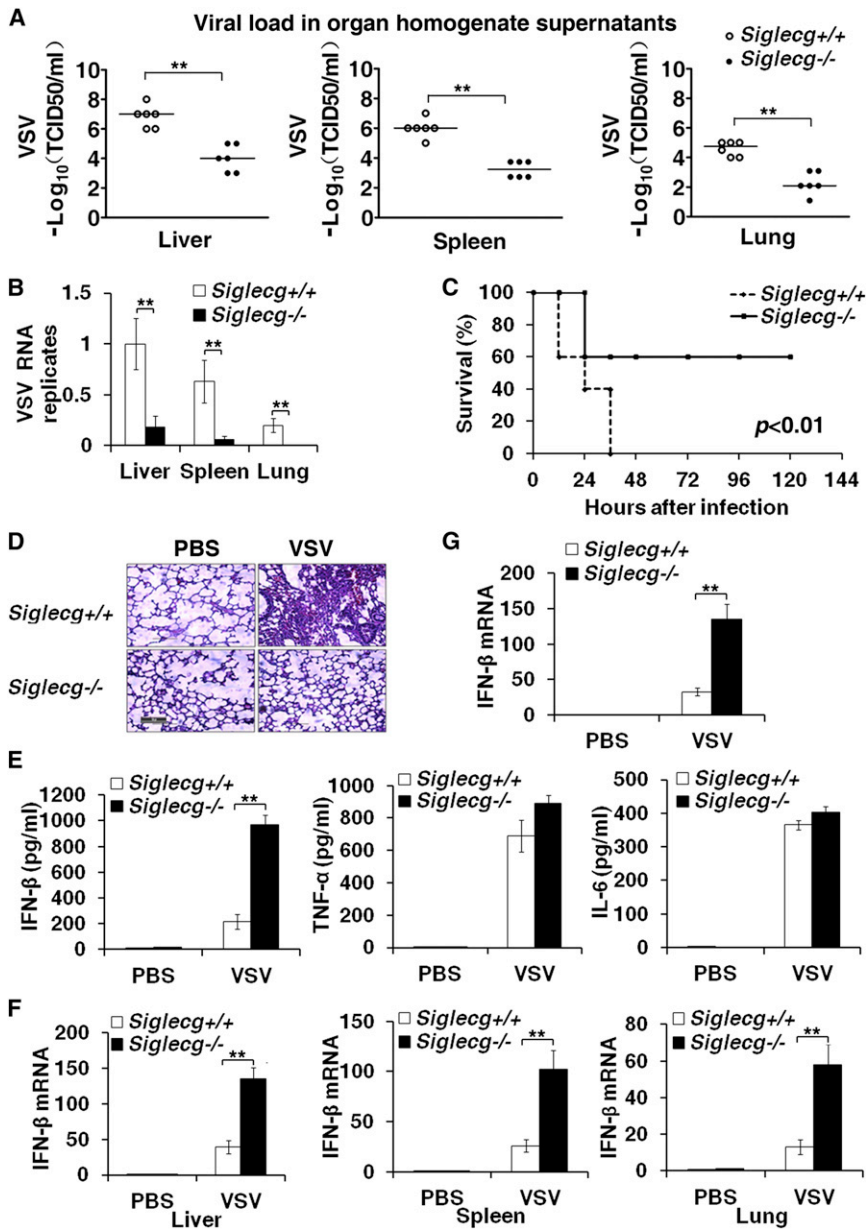


Figure 2. *Siglec*G-Deficient Mice Are More Resistant to RNA Viral Infection by Producing More IFN- β

(A) Determination of VSV loads in organs by TCID_{50} assay 24 hr after $\text{Siglec}^{+/+}$ and $\text{Siglec}^{-/-}$ mice ($n = 6$ per group) were intraperitoneally injected with VSV.

(B) Q-PCR analysis of VSV expression in organs from $\text{Siglec}^{+/+}$ and $\text{Siglec}^{-/-}$ mice in (A).

(C) Survival of ~ 7 -week-old $\text{Siglec}^{+/+}$ and $\text{Siglec}^{-/-}$ mice given intraperitoneal injection of VSV (1×10^8 pfu/g) ($n = 10$ per group). $p < 0.01$.

(D) Pathology of $\text{Siglec}^{+/+}$ and $\text{Siglec}^{-/-}$ mice in response to VSV. Scale bar, 100 μm . Hematoxylin and eosin staining of lung sections from mice in (A).

(E) ELISA of cytokine production in sera from $\text{Siglec}^{+/+}$ and $\text{Siglec}^{-/-}$ mice in (A).

(F) Q-PCR analysis of IFN- β mRNA expression in organs from $\text{Siglec}^{+/+}$ and $\text{Siglec}^{-/-}$ mice in (A).

(G) Q-PCR analysis of IFN- β mRNA expression in peritoneal macrophages from $\text{Siglec}^{+/+}$ or $\text{Siglec}^{-/-}$ mice in (A).

Data are means \pm SEM. $**p < 0.01$. See also Figure S2.

poly(I:C), and LM or transfected with poly(dA:dT) or poly(dG:dC) (Figure S3E). We further confirmed that siRNA knock-down of *Siglec*G significantly increased the production of IFN- β and mRNA expression of IFN- β and IFN- $\alpha 4$ in macrophages infected with VSV or SeV (Figures 3C–3E). Furthermore, RAW264.7 macrophages with Flag-tagged Siglec-G stably overexpressed produced less IFN- β and expressed lower IFN- β and IFN- $\alpha 4$ mRNA in response to infection with VSV or SeV, but not HSV-1 (Figures 3F–3H). Correspondingly, virus replication was more significantly inhibited in $\text{Siglec}^{-/-}$ macrophages infected with VSV (Figure 3I), and enhanced viral replication was observed in Siglec-G-overexpressing RAW264.7

macrophages infected with VSV (Figure 3J). These data suggest that Siglec-G selectively suppresses production of type I interferon and inhibits antiviral innate response against RNA viral infection.

Siglec Deficiency Enhances IRF3 Activation by RNA Viral Infection through the RIG-I Pathway

We further investigated the effect of *Siglec*G deficiency on RNA virus activated downstream signal pathways in macrophages. We found that phosphorylation of IKK and IRF3 was markedly enhanced in $\text{Siglec}^{-/-}$ macrophages compared with $\text{Siglec}^{+/+}$ macrophages after VSV infection. By contrast, we did not observe an appreciable difference in p65, p38, ERK, and JNK phosphorylation between $\text{Siglec}^{-/-}$ and

Siglec-G Selectively Inhibits RNA-Virus-Induced Type I Interferon Production in Macrophages and Dendritic Cells

Upon infection with VSV or SeV, but not HSV-1, $\text{Siglec}^{-/-}$ macrophages produced more IFN- β , TNF- α , and IL-6 protein and expressed higher IFN- β and IFN- $\alpha 4$ mRNA than $\text{Siglec}^{+/+}$ macrophages (Figures 3A, 3B and S3A). The same phenomenon was also observed in bone-marrow-derived dendritic cells (BMDCs) (Figures S3B and S3C). As to the response to TLR ligands, $\text{Siglec}^{-/-}$ macrophages produced IFN- β more obviously than $\text{Siglec}^{+/+}$ macrophages in response to intracellular transfection of poly(I:C) (Figure S3D). By contrast, no difference in IFN- β secretion was observed between $\text{Siglec}^{-/-}$ and $\text{Siglec}^{+/+}$ macrophages stimulated with LPS, R837,

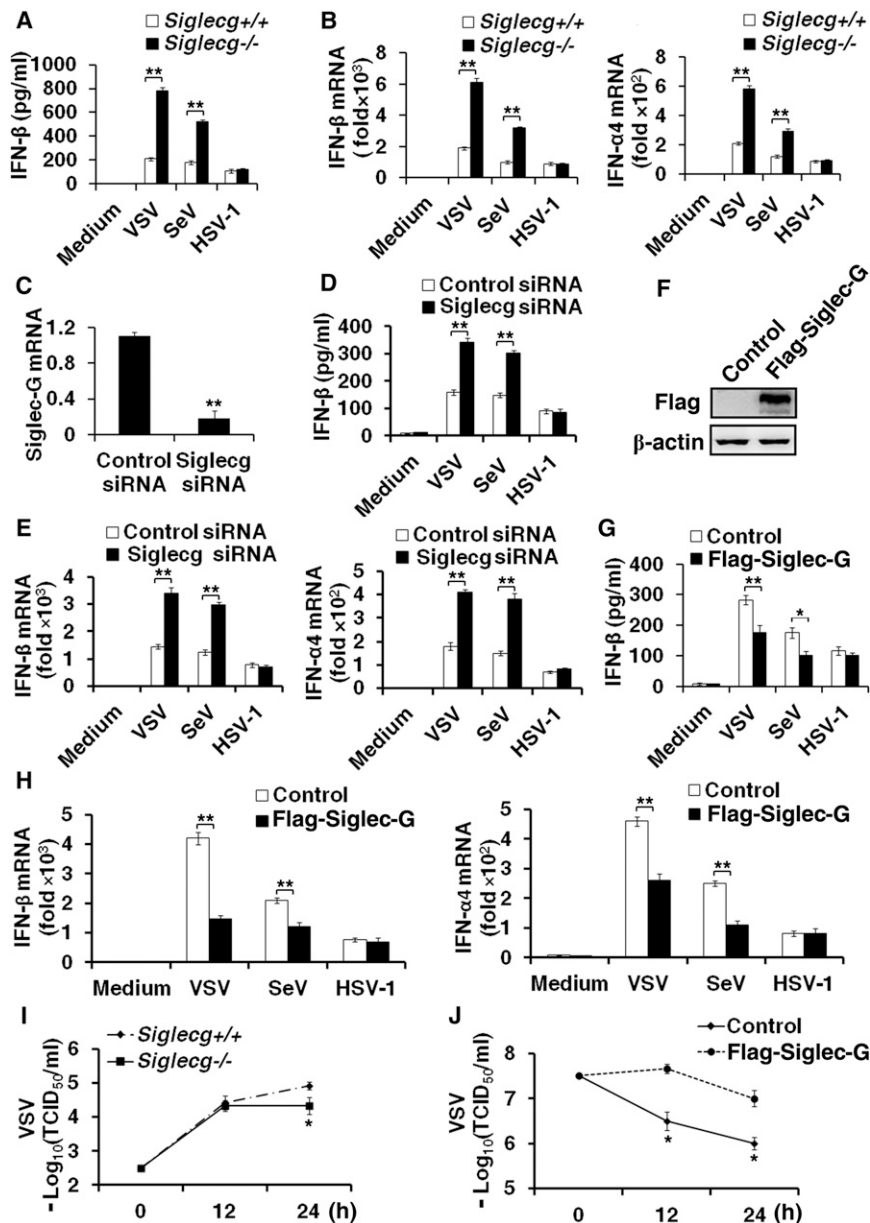


Figure 3. Siglec-G Selectively Inhibits RNA-Virus-Induced Production of Type I Interferon in Macrophages

(A) ELISA of IFN-β in supernatants of *Siglecg*^{+/+} and *Siglecg*^{-/-} peritoneal macrophages infected for 24 hr with VSV, SeV, or HSV-1.

(B) Q-PCR analysis of IFN-β and IFN-α4 mRNA expression in *Siglecg*^{+/+} and *Siglecg*^{-/-} macrophages infected for 8 hr with VSV, SeV, or HSV-1.

(C) Q-PCR analysis of Siglec-G mRNA expression in macrophages 48 hr after transfection with Siglec-G siRNA.

(D) ELISA of IFN-β in supernatants of macrophages transfected as in (C) and 48 hr later infected for 24 hr with VSV, SeV, or HSV-1.

(E) Q-PCR analysis of IFN-β and IFN-α4 mRNA expression in macrophages transfected as in (C) and 48 hr later infected for 8 hr with VSV, SeV, or HSV-1.

(F) Immunoblot analysis of Siglec-G expression in Siglec-G-overexpressing RAW264.7 macrophages with α-Flag.

(G) ELISA of IFN-β in supernatants of Siglec-G-overexpressing RAW264.7 macrophages infected for 24 hr with VSV, SeV, or HSV-1.

(H) Q-PCR analysis of IFN-β and IFN-α4 mRNA expression in Siglec-G-overexpressing RAW264.7 macrophages infected for indicated time with VSV, SeV, or HSV-1.

(I) Determination of VSV titers in supernatants of *Siglecg*^{+/+} and *Siglecg*^{-/-} peritoneal macrophages changed culture medium for indicated hours after VSV infection for 8 hr by TCID₅₀ assay.

(J) Determination of VSV titers in supernatants of Siglec-G-overexpressing RAW264.7 macrophages infected for indicated hours with VSV by TCID₅₀ assay.

Data are means ± SEM. *p < 0.05; **p < 0.01. See also Figure S3.

Siglecg^{+/+} macrophages (Figures 4A and 4B). Deficiency in *Siglecg* resulted in more VSV-induced nuclear translocation of IRF3 (Figure 4C). Moreover, deficiency in *Siglecg* maintained higher expression of RIG-I at basal level and increased RIG-I protein expression in macrophages after infection with VSV (Figure 4D) or SeV (Figure S4A). However, little or no difference in expression of MAVS was detected (Figures 4D and S4A). We also observed that expression of Siglec-G protein was upregulated in *Siglecg*^{+/+} macrophages with VSV infection for 16 hr, and RIG-I protein level was lower at the time point (Figure 4E). Phosphorylation of IRF3 was decreased with lower expression of RIG-I after VSV or SeV infection in Siglec-G-overexpressing RAW264.7 macrophages compared to control cells (Figures 4F and S4B). The cyclohex-

RNA-virus-induced IRF3 activation by reducing RIG-I protein expression accordingly.

Siglec-G Promotes c-Cbl-Mediated Ubiquitination and Degradation of RIG-I

To investigate the underlying mechanisms involved in the negative regulation of RIG-I pathway by Siglec-G, we immunoprecipitated Siglec-G from lysates of VSV-infected RAW264.7 macrophages stably overexpressing Flag-Siglec-G with an antibody against the Flag epitope tag and then used mass spectrometry to identify Siglec-G-associated proteins. Among the Siglec-G-interacting proteins detected in the immunoprecipitates, we focused on E3 ligases in the data set for their possibility in regulating RIG-I turnover. A total of three E3 ligases

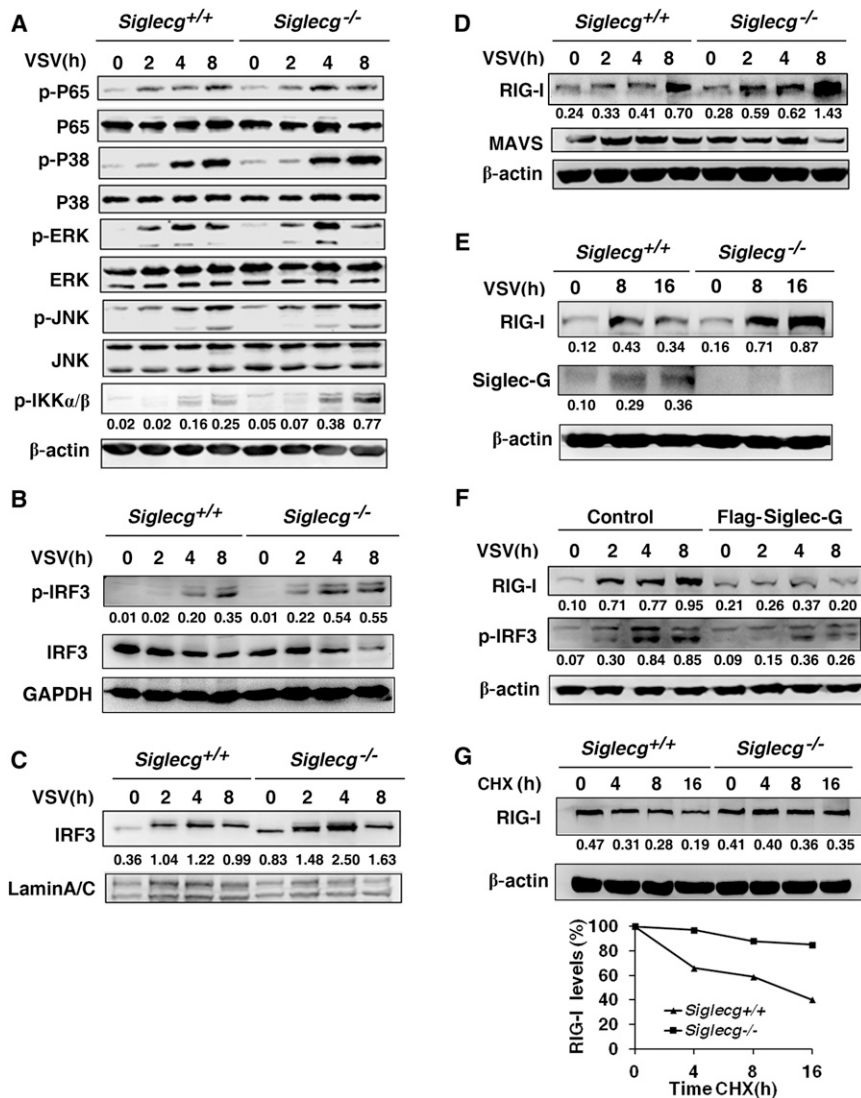


Figure 4. SiglecG Deficiency Enhances IRF3 Activation in RNA-Virus-Infected Macrophages with Higher Expression of RIG-I

(A and B) Immunoblot analysis of phosphorylated (p-) or total proteins in lysates of *Siglecg*^{+/+} or *Siglecg*^{-/-} peritoneal macrophages infected for indicated hours with VSV.

(C) Immunoblot analysis of IRF3 among nuclear proteins from *Siglecg*^{+/+} or *Siglecg*^{-/-} macrophages infected with VSV; lamin A/C serves as a loading control.

(D) Immunoblot analysis of RIG-I and MAVS in lysates of *Siglecg*^{+/+} or *Siglecg*^{-/-} macrophages infected with VSV.

(E) Immunoblot analysis of RIG-I and Siglec-G in lysates of *Siglecg*^{+/+} or *Siglecg*^{-/-} macrophages infected with VSV.

(F) Immunoblot analysis of RIG-I and p-IRF3 in lysates of Siglec-G-overexpressing RAW264.7 macrophages infected with VSV.

(G) Immunoblot analysis of RIG-I in lysates of *Siglecg*^{+/+} or *Siglecg*^{-/-} macrophages treated with CHX (100 mg/ml) for indicated hours after infection with VSV for 2 hr. Quantification of relative RIG-I levels is shown in the bottom panel. Numbers below lanes (top) indicate densitometry of the protein presented relative to β -actin or GAPDH expression in that same lane (below).

See also Figure S4.

were identified as putative Siglec-G-binding proteins, and we chose to study c-Cbl first, given that it has the highest Mascot scores and the highest number of matched peptides (Figure S5A). We observed that the level of ubiquitination conjugated to RIG-I was low in the absence of ectopic c-Cbl expression (Figure 5A), and the levels of RIG-I were reduced as increasing amounts of c-Cbl were expressed. When cells were treated with the proteasome inhibitor MG132, the degradation of RIG-I was suppressed (Figure 5B). Under these conditions, RIG-I expression was further reduced in the presence of Siglec-G (Figure 5C). Knocking down c-Cbl with specific siRNA in macrophages increased the half-life of endogenous RIG-I protein during VSV infection (Figure S5B). These results suggest that Siglec-G functionally promotes c-Cbl to regulate the levels of RIG-I protein through proteasomal degradation.

Considering that the activated Siglec-G has ITIMs capable of recruiting the tyrosine phosphatase SHP2, we investigated

whether the tyrosine residues of Siglec-G were phosphorylated and whether Siglec-G promotes c-Cbl to regulate the RIG-I pathway via SHP2 upon RNA virus infection. At 1 hr after Siglec-G-overexpressing RAW264.7 macrophages were infected with VSV, tyrosine phosphorylation of Siglec-G increased markedly (Figure 5D). At 8 hr after VSV infection, there was much less phosphorylation of c-Cbl and SHP2 in *Siglecg*^{-/-} macrophages than in *Siglecg*^{+/+} macrophages (Figure 5E). The IFN- β mRNA expression increased in VSV-infected macrophages treated with specific siRNA for c-Cbl or SHP2 (Figures 5F and 5G). Similar observations were made in Siglec-G-overexpressing RAW264.7 macrophages (Figures S5C and S5D). On the contrary, the IFN- β mRNA expression was attenuated in c-Cbl-overexpressing RAW264.7 macrophages infected with VSV (Figure S5E). We further found that knocking down c-Cbl with siRNA could up-regulate IFN- β mRNA expression in *shp2*^{-/-} macrophages with VSV infection. Interfering Siglec-G expression in *shp2*^{-/-} macrophages with VSV infection did not affect IFN- β production (Figure 5H), suggesting that SHP2 might function upstream of c-Cbl in this pathway. CD24 and some sialic acids are known as ligands for Siglec-G (Chen et al., 2009). Using *CD24*^{-/-} mice, we found that CD24 deficiency did not affect VSV-induced *Siglecg* expression and IFN- β production in macrophages (Figures S5F–S5H). And knocking down Siglec-G with siRNA still could increase the production of IFN- β in CD24-deficient

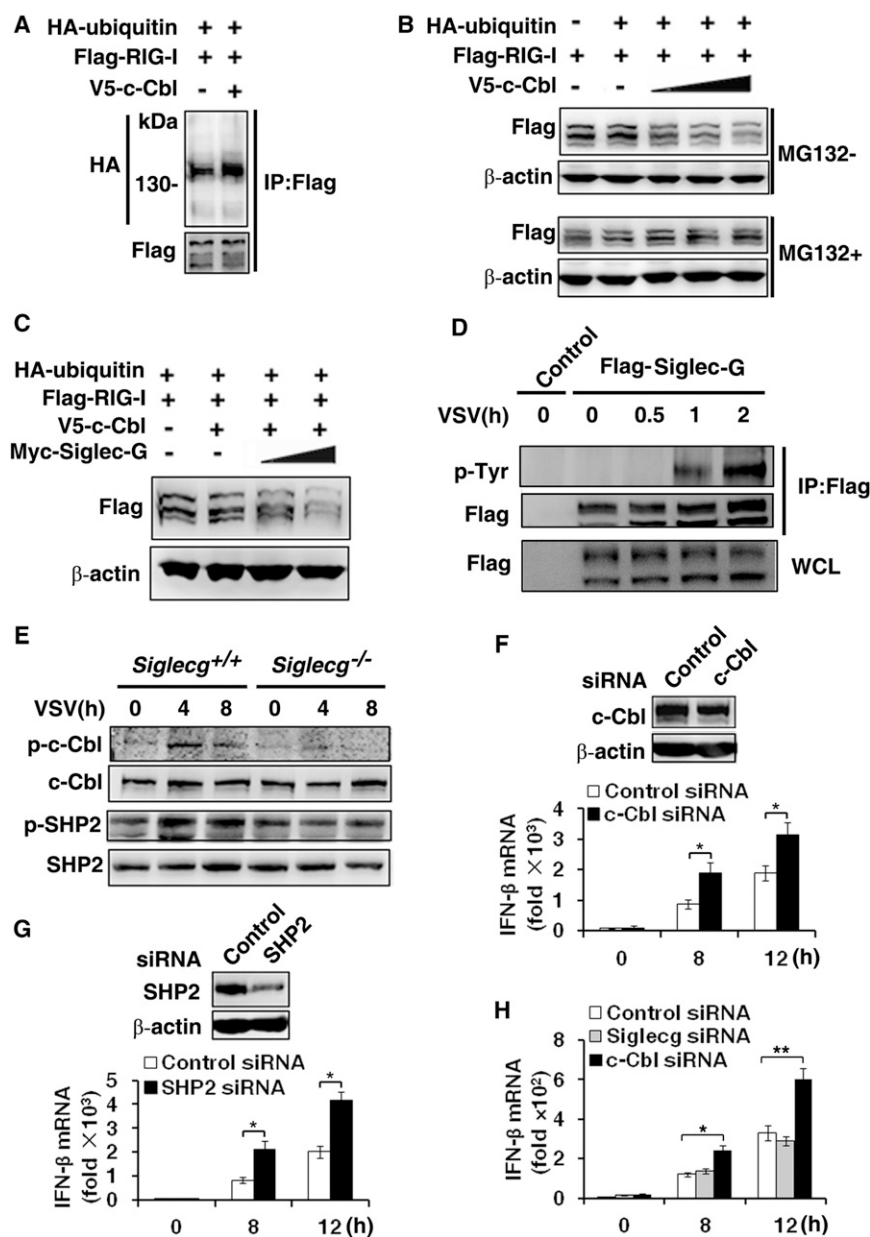


Figure 5. Siglec-G Promotes c-Cbl-Mediated Degradation of RIG-I via SHP2

(A) c-Cbl is an E3 ligase for ubiquitin to RIG-I. Plasmids encoding Flag-RIG-I and HA-ubiquitin were cotransfected into HEK293T cells with or without a plasmid encoding V5-c-Cbl. The RIG-I ubiquitination was monitored by immunoprecipitation. All cells were treated with MG132 (10 μ M). (B) c-Cbl mediates RIG-I degradation in a proteasome-dependent manner. The HEK293T cells were transfected with plasmids encoding Flag-RIG-I, HA-ubiquitin, and varying doses of a plasmid encoding V5-c-Cbl (0.5, 1.0, and 1.5 μ g). Half of each cell aliquot was treated with MG132 (10 μ M). The level of RIG-I protein was examined in cells harvested 24 hr after transfection.

(C) Siglec-G promotes c-Cbl-mediated degradation of RIG-I in a dose-dependent manner. The HEK293T cells were transfected with plasmids encoding Flag-RIG-I, HA-ubiquitin, V5-c-Cbl, and varying doses of a plasmid encoding Myc-Siglec-G (0.5 and 1 μ g). The level of RIG-I protein was examined in cells harvested 24 hr later.

(D) VSV infection induces tyrosine phosphorylation of Siglec-G. Flag-Siglec-G-overexpressing RAW264.7 macrophages were infected with VSV for the indicated hours. Immunoblot analysis of phosphorylated tyrosine (p-Tyr) protein in cell lysates immunoprecipitated with antibody to Flag tag.

(E) Siglec-G promotes phosphorylation of c-Cbl and SHP2. Immunoblot analysis of phosphorylated (p-) c-Cbl and p-SHP2 protein in lysates of *Siglecg*^{-/-} or *Siglecg*^{+/+} macrophages infected with VSV.

(F and G) Siglec-G inhibits IFN- β production through c-Cbl or SHP2. Q-PCR analysis of IFN- β mRNA expression in macrophages transfected with c-Cbl siRNA (F) or SHP2 siRNA (G) and 48 hr later infected for indicated hours with VSV.

(H) SHP2 functions upstream of c-Cbl in Siglec-G inhibition of IFN- β production. Q-PCR analysis of IFN- β mRNA expression in *shp2*^{-/-} macrophages transfected with Siglec-G siRNA or c-Cbl siRNA and 48 hr later infected for indicated hours with VSV.

Data are means \pm SEM. * p < 0.05. See also Figure S5.

macrophages infected with VSV (Figure S5I). Sialidase treatment did not affect the phenotype of the increased IFN- β production in *Siglecg*^{-/-} macrophages upon VSV infection (Figure S5J). These findings demonstrate that Siglec-G promotes c-Cbl-mediated degradation of RIG-I via SHP2 to regulate RNA-virus-induced type I IFN production.

Siglec-G Associates with SHP2, c-Cbl, and RIG-I

Coimmunoprecipitation experiments revealed that Siglec-G interacts with c-Cbl/SHP2/RIG-I, and RIG-I interacts with c-Cbl/SHP2/Siglec-G in various tagged plasmids coexpressed in HEK293T cells (Figure 6A). Interaction between Flag-tagged Siglec-G and endogenous RIG-I/c-Cbl/SHP2 was readily de-

tected in Siglec-G-overexpressing RAW264.7 macrophages infected with VSV (Figure 6B). Furthermore, the endogenous Siglec-G/RIG-I/c-Cbl/SHP2 complex was also detected in VSV-infected peritoneal macrophages from *Siglecg*^{+/+} mice. However, the association was almost undetected in VSV-infected peritoneal macrophages from *Siglecg*^{-/-} mice (Figure 6C). Confocal microscopy also revealed that intracellular RIG-I localized together with c-Cbl and Siglec-G in cytoplasm of HEK293T cells 6 hr after infection with SeV (Figure 6D).

Siglec-G contains four ITIM motifs in the intercellular domain. Binding analysis revealed that the Siglec-G (4YF) mutant interacted to RIG-I much more weakly than full-length Siglec-G, whereas the cytoplasmic domain-deleted Siglec-G mutant did

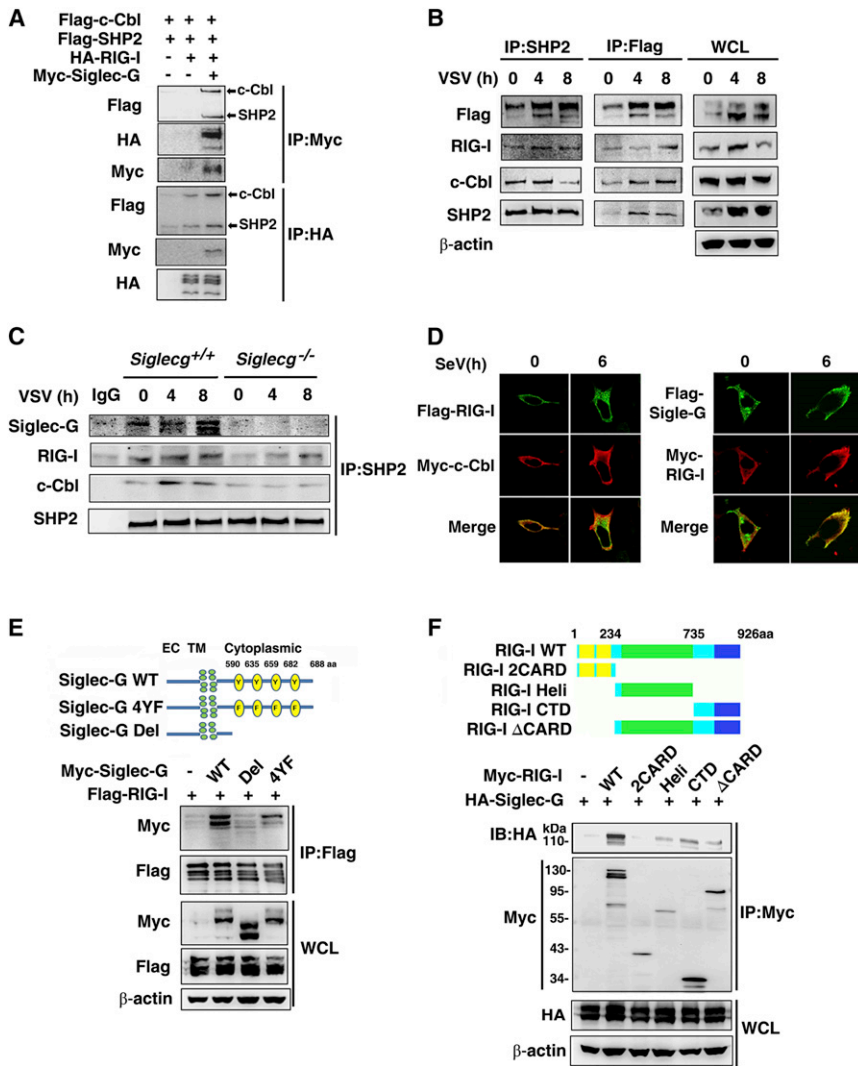


Figure 6. Siglec-G Interacts with SHP2, c-Cbl, and RIG-I

(A) Protein complex of Siglec-G, SHP2, c-Cbl, and RIG-I in overexpressing system. The HEK293T cells were transfected for 24 hr with plasmids encoding HA-RIG-I, Flag-SHP2, Flag-c-Cbl, and Myc-Siglec-G. Immunoblot analysis of Myc-Siglec-G, HA-RIG-I, Flag-SHP2, or Flag-c-Cbl immunoprecipitated with antibodies to myc or HA tags.

(B) Protein complex of Flag-Siglec-G, SHP2, c-Cbl, and RIG-I in macrophages. Siglec-G-overexpressing RAW264.7 macrophages were infected with VSV for indicated hours. Immunoblot analysis of endogenous RIG-I, SHP2, or c-Cbl immunoprecipitated with antibody to SHP2 or Flag tag.

(C) Interaction of Siglec-G, c-Cbl, and RIG-I with SHP2 in peritoneal macrophages. *Siglecg^{-/-}* or *Siglecg^{+/+}* macrophages were infected with VSV for indicated hours. Immunoblot analysis of endogenous Siglec-G, RIG-I, c-Cbl, or SHP2 immunoprecipitated with antibody to SHP2. IgG was as control.

(D) Confocal microscopy of HEK293T infected for 6 hr with SeV. HEK293T cells were transfected with Flag-RIG-I, Myc-c-Cbl, Flag-Siglec-G, or Myc-RIG-I for 24 hr and then infected with SeV and labeled with antibodies to the appropriate molecules.

(E) Intracellular domain of Siglec-G associates with RIG-I. Schematic structure of Siglec-G and the derivatives used were shown (top). WCLs of HEK293T cells transfected with Myc-Siglec-G (WT), Myc-Siglec-G (Del), Myc-Siglec-G (4YF), and Flag-RIG-I were used for immunoprecipitation and immunoblotting, as indicated.

(F) Siglec-G associates with the Helix/CTD of RIG-I. Schematic structure of RIG-I and the derivatives used were shown (top). WCLs of HEK293T cells transfected with Myc-RIG-I (WT), Myc-RIG-I (2CARD), Myc-RIG-I (Heli), Myc-RIG-I (CTD), or with Myc-RIG-I (Δ CARD) and HA-Siglec-G were used for immunoprecipitation and immunoblotting, as indicated.

not interact with RIG-I (Figure 6E). Coexpressing plasmids in HEK293T revealed that SHP2 promoted Siglec-G interaction with RIG-I (Figure S6A), indicating that ITIM motifs of Siglec-G are important for Siglec-G to associate with RIG-I through recruiting SHP2. To determine which domain of RIG-I was required for the interaction of RIG-I with Siglec-G or c-Cbl, we constructed mutants of RIG-I with the deletion of various domains and found that Heli or/and CTD domain of RIG-I interacted with Siglec-G (Figure 6F) and CTD domain of RIG-I associated with c-Cbl (Figure S6B).

Lys813 Is a Critical Site in c-Cbl-Mediated K48-Linked Ubiquitination of RIG-I

Based on c-Cbl-mediated ubiquitination and degradation of RIG-I, we analyzed K48-linked ubiquitin to RIG-I, and found that Siglec-G promoted c-Cbl-mediated K48-linked ubiquitination and degradation of RIG-I in a dose-dependent manner (Figures 7A, 7B, S7A, S7B, S7D, and S7E). c-Cbl did not

substantially affect K63-linked ubiquitination and degradation of RIG-I (Figures S7E and S7F).

We further analyzed the most conserved lysine residues of RIG-I among different species and constructed those plasmids in which lysine residues were replaced with arginine (K→R) individually (data not shown). The K813R mutation caused near-complete loss of K48 ubiquitination and degradation of RIG-I (Figures 7C, 7D, S7C, and S7G). Transfection of RIG-I-K813R induced IFN- β promoter activation more markedly in HEK293T cells, consistent with their lack of ubiquitination and degradation of RIG-I (Figure 7E). Furthermore, VSV infection induced much more IFN- β mRNA expression in RIG-I-K813R-overexpressing RAW264.7 macrophages than in wild-type RIG-I-overexpressing RAW264.7 macrophages (Figure S7H). In RIG-I-deficient peritoneal macrophages, transfection of the RIG-I-K813R mutant restored VSV-induced IFN- β expression significantly more than transfection of wild-type RIG-I (Figure 7F). These results suggest that Lys813 of RIG-I

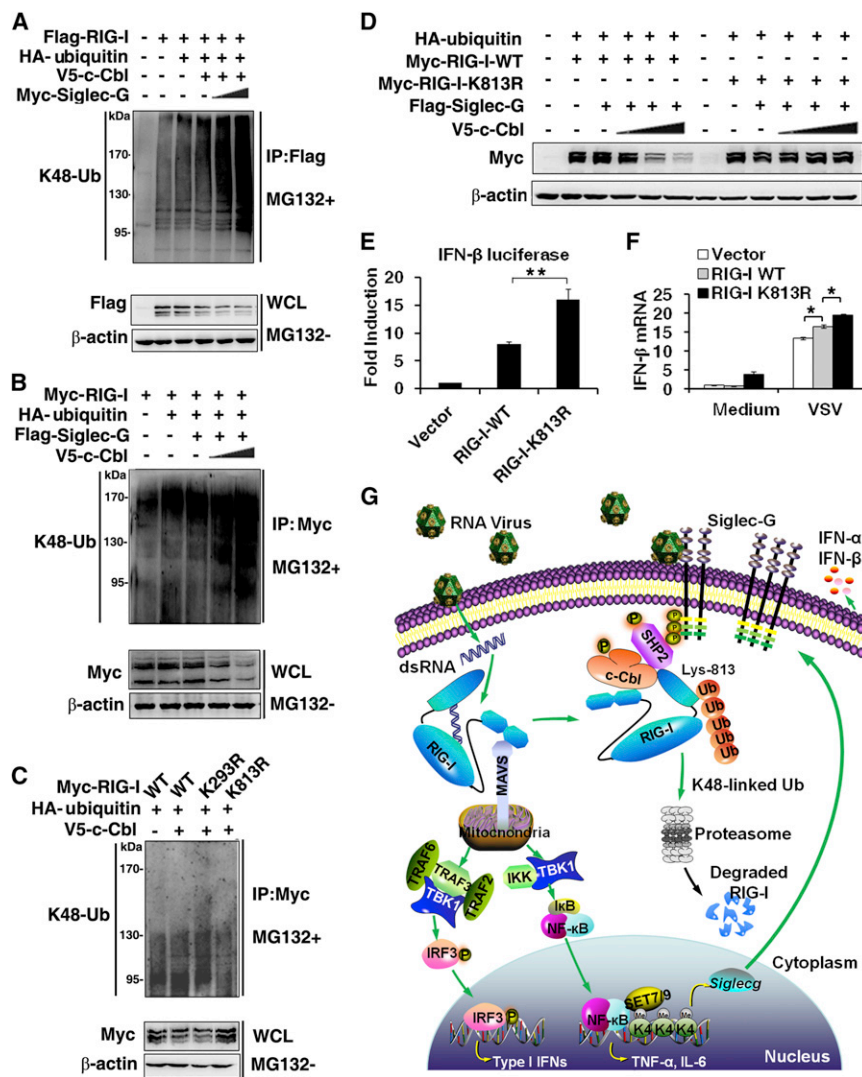


Figure 7. Lys813 of RIG-I Is a Critical Site in c-Cbl-Mediated K48-Linked Ubiquitination and Degradation of RIG-I

(A) Siglec-G promotes c-Cbl-mediated K48-linked ubiquitination of RIG-I. The HEK293T cells were transfected with plasmids encoding Flag-RIG-I, HA-ubiquitin, V5-c-Cbl, and varying doses of a plasmid encoding Myc-Siglec-G (0, 0.5, and 1 μg). Half of each cell aliquot was treated with MG132 (10 μM). Cells were harvested 24 hr after transfection for immunoblot analysis of K48-Ub immunoprecipitated with antibody to Flag tag.

(B) c-Cbl mediates K48-linked ubiquitination of RIG-I in a dose-dependent way. The HEK293T cells were transfected with plasmids encoding Myc-RIG-I, HA-ubiquitin, Flag-Siglec-G, and varying doses of a plasmid encoding V5-c-Cbl (0, 0.5, and 1 μg). Half of each cell aliquot was treated with MG132 (10 μM). Cells were harvested 24 hr after transfection for immunoblot analysis of K48-Ub immunoprecipitated with antibody to myc tag.

(C) K813 of RIG-I is the major site of c-Cbl-mediated K48-linked ubiquitination. WCLs of HEK293T cells transfected with HA ubiquitin, V5-c-Cbl, Myc-RIG-I (WT), or K→R mutants were used for immunoprecipitation and immunoblot analysis of K48-Ub. Half of each cell aliquot was treated with MG132 (10 μM).

(D) K813 is critical site in c-Cbl-mediated degradation of RIG-I. WCLs of HEK293T cells transfected with V5-c-Cbl, HA-ubiquitin, Flag-Siglec-G, Myc-RIG-I WT, or K813R mutants were used for immunoblot analysis of RIG-I with antibody to myc tag.

(E) *IFN-β* promoter activity in RIG-I-WT or RIG-I-K813R-transfected HEK293T cells detected by luciferase reporter assay. Luciferase activity was analyzed as fold induction. Data are means ± SEM. **p < 0.01.

(F) Q-PCR analysis of *IFN-β* mRNA expression in *Rigi*^{-/-} macrophages transfected with RIG-I-WT or RIG-I-K813R plasmid and 24 hr later infected for 8 hr with VSV. Data are means ± SEM. *p < 0.05.

(G) Model of the RNA-virus-activated Siglec-G-SHP2-c-Cbl-mediated RIG-I degradation. Upon RNA virus infection, Siglec-G is activated, and then its phosphorylated ITIMs recruit tyrosine phosphatase SHP2. Siglec-G promotes phosphorylation of SHP2 and c-Cbl. RIG-I is also recruited and associated with Siglec-G-SHP2-c-Cbl, leading to K48-linked ubiquitination and proteasomal degradation of RIG-I by E3 ligase c-Cbl. Lys813 of RIG-I is a critical site for c-Cbl-mediated RIG-I degradation. On the other hand, RNA virus infection triggers RIG-I downstream signal activation through RIG-I-MAVS interaction, and the activated NF-κB upregulates Siglec-G mRNA expression, which inhibits RIG-I-triggered type I interferon production in the innate immune response, forming a negative feedback loop.

See also Figure S7.

is an important site for K48 ubiquitination and degradation of RIG-I.

DISCUSSION

RLR signaling is regulated at multiple steps in the signaling cascade. The helicase and repressor domain (RD) of RIG-I bind RNA ligands, leading to a conformational change that releases CARDs from RD repression, activating signaling (Jiang et al., 2011; Kowalinski et al., 2011). During virus infection, ATP and dsRNA binding induces a major rearrangement, creating a closed conformation in which the helicase and CTD bind

dsRNA. This co-operative tight binding liberates the CARDs for downstream signaling. The CARDs interact with the adaptor protein MAVS/IPS-1/VISA/Cardif to form a MAVS signalosome that drives type I IFN production (Kowalinski et al., 2011; Seth et al., 2005; Hou et al., 2011; O'Neill and Bowie, 2011). Negative regulators of RIG-I signaling pathway include deubiquitinases such as CYLD, which interact with the CARDs of RIG-I to remove K63-linked polyubiquitin chains and inhibit downstream signaling (Friedman et al., 2008). However, only RNF125 E3 ligase has thus far been reported to mediate polyubiquitination and degradation of RIG-I (Arimoto et al., 2007). Further investigation will be required to identify additional ubiquitination sites and

other ubiquitin ligases or proteins that can regulate RIG-I signaling. Here, we have shown that Siglec-G, upregulated by RNA virus, promotes c-Cbl-mediated K48-linked ubiquitination on Lys813 of RIG-I and subsequent degradation of RIG-I. To our knowledge, this is the first report of K48-linked ubiquitination of RIG-I and also the critical site (Lys813) of RIG-I for ubiquitination and degradation. Our results, showing that overexpressed RIG-I-K813R is quite stable in HEK293 cells in which RNF125 and other E3 ligases also express, indicate that Lys813 may also be a ubiquitination site for RNF125 or the key site for K48-linked ubiquitination of RIG-I by all others E3 ligases. Thus, our study provides a new manner for negative regulation of RIG-I at the posttranslational level and identifies a previously unknown function of E3 ligase c-Cbl that could mediate proteasomal degradation of RIG-I.

Cbls (c-Cbl, Cbl-b, and Cbl-c) are single-subunit RING E3s that negatively regulate a host of proteins by promoting their ubiquitination and subsequent degradation by the proteasome or through endocytosis (Joazeiro et al., 1999; Schmidt and Dikic, 2005). The ligase activity of human c-Cbl is regulated by Try371 phosphorylation to break autoinhibition (Dou et al., 2012), but the phosphorylated tyrosine site of murine c-Cbl for activation is not clear. Here, we have shown that a higher Try731 phosphorylation level of murine c-Cbl occurred in *Siglecg*^{+/+} macrophage compared to *Siglecg*^{-/-} macrophage upon VSV infection, which may promote c-Cbl activation. Given reports that c-Cbl is associated with SHP2 following stimulation by SDF-1 (Chernock et al., 2001) and that the c-Cbl/SHP2 complex is involved in ubiquitination and degradation of gp130 upon IL-6 stimulation (Tanaka et al., 2008), we detected an interaction between RIG-I and c-Cbl via SHP2. Our data showed that recruiting of SHP2 by Siglec-G is involved in c-Cbl-mediated negative regulation of RIG-I signaling for type I IFN production. Thus, the precise mechanism of c-Cbl activation and relationship between c-Cbl and SHP2 need further investigation. Our lab previously reported that SHP2 negatively regulates MyD88 and TRIF-mediated gene expression in TLR signaling, in part by interfering with TRAF6-mediated signaling and through inhibition of TBK1-activated signal transduction (An et al., 2006; Xu et al., 2012). By showing a critical role for SHP2 in RLR regulation, we extended the function of SHP2 into PRRs known to be involved in regulating viral infection.

Siglec-G belongs to a superfamily of immunoglobulin-like lectins defined by their ability to recognize sialic-acid-containing structures, functioning as a negative regulator of BCR-mediated signaling and an inhibitory receptor of B1 cells. Although CD24 and some sialic acids are known as ligands for Siglec-G (Chen et al., 2009), we confirmed that negative function of Siglec-G in VSV-induced IFN- β production is not dependent on its interaction with CD24 molecule or other sialic acids presented on the cell surface of macrophages. We speculated that sialic acids of viral glycoproteins, but not sialic acids on the surface of macrophages, might be recognized by Siglec-G and then trigger the downstream signal. The tyrosines within the ITIM of Siglec-G become phosphorylated by following ligation of the receptors and recruit SHP1/2 to regulate cellular activity (Crocker et al., 2007). However, the regulation of Siglec-G expression and its roles in innate immunity are unclear. Consistent with the observation that Siglec-G deficiency did not affect the production of

inflammatory cytokines by DCs in response to LPS or poly(I:C) (Chen et al., 2009), our finding that Siglec-G inhibits induction of type I IFN production by RNA virus infection in macrophages may provide new insight into the biological function of Siglec-G in innate immunity.

TLRs are key sensors that trigger signaling cascades to activate inflammatory programs via the NF- κ B gene network. Interestingly, NF- κ B, activated by RIG-I but not TLRs, could upregulate Siglec-G expression. We found that LPS stimulation did not affect the significantly increased H3K4me3 and/or decreased H3K27me3 levels in macrophages infected by VSV. The data revealed a functional link between regulation of gene expression and epigenetic control of NF- κ B signaling in the regulation of innate immunity. The phenomenon also opens a gate to how a virus can escape immune attack and survive by upregulating Siglec-G through epigenetic modification.

Here, we have shown that Siglec-G is specifically upregulated by RNA virus infection and regulates RIG-I signaling in macrophages through a negative feedback mechanism. Consequently, Siglec-G suppresses type I IFN production by promoting c-Cbl-mediated K48-linked ubiquitination and proteasomal degradation of RIG-I. This process depends on phosphorylation of SHP2 and c-Cbl, as illustrated in Figure 7G. This working model explains why *Siglecg*-deficient mice show more resistance to RNA virus infection. These findings provide insight into the negative regulation of RIG-I-mediated antiviral innate immune responses, a mechanistic explanation for the immunological escape of RNA virus, and potential therapeutic targets for virus-associated inflammatory diseases.

EXPERIMENTAL PROCEDURES

Plasmids, cells, pathogens, antibodies, ELISA kits, and other reagents used, as well as detailed experimental procedures can be found in the [Extended Experimental Procedures](#).

Mice

Siglecg^{-/-} and *CD24*^{-/-} mice on a C57BL/6J background were generated as described previously (Ding et al., 2007; Nielsen et al., 1997). *Rigi*^{-/-} mice on a 129/Sv/C57BL/6J background were kindly provided by Dr. Zhugang Wang (Wang et al., 2007). *Shp2*^{fl} mice were a kind gift from Dr. Gensheng Feng. Mx-Cre mice and mice deficient in *Irf3*, *Irf β* , and *Irf α β r* were from Jackson Laboratories. C57BL/6J mice were purchased from Joint Ventures Sipper BK Experimental Animals (Shanghai, China). Mice were kept and bred in pathogen-free conditions. All animal experiments were undertaken in accordance with the National Institute of Health Guide for the Care and Use of Laboratory Animals with approval of the Scientific Investigation Board of Second Military Medical University, Shanghai.

Coimmunoprecipitation, Immunoblot Analysis, RT-PCR, RNAi, Luciferase Reporter Assay, and VSV TCID₅₀ Assay

These experiments were performed as described previously (Hou et al., 2009; Yang et al., 2010; Liu et al., 2011).

Immunofluorescent Confocal Microscopy

The experiments were performed as described previously (Xu et al., 2012). Imaging of the cells was carried out using Leica TCS SP2 confocal laser microscopy under a 100 \times oil objective.

Microarray Analysis

Total RNA was isolated using an RNA isolation kit (QIAGEN) and was verified with RNA integrity number (RIN). Whole-genome-wide expression

analysis was performed with Affymetrix Mouse Genome 430 2.0 Arrays. Differentially expressed genes were identified using Limma (Bioconductor package) in R software. Detailed procedures are described in the [Extended Experimental Procedures](#).

Lung Histology

Lungs from control or virus-infected mice were dissected, fixed in 10% phosphate-buffered formalin, embedded into paraffin, sectioned, stained with hematoxylin and eosin solution, and examined by light microscopy for histological changes. Immunohistochemical staining was performed using standard procedures.

Isolation of Macrophages and BMDCs

Peritoneal macrophages were harvested from mice 4 days after thioglycolate (BD, Sparks, MD) injection. BMDCs from C57BL/6J mice were generated as described previously (Liu et al., 2011). Cells were plated into 12-well plates and cultured in the absence or presence of LPS (100 ng/ml), CpG ODN(0.3 μ M), R837(10 μ g/ml), poly(I:C) (10 μ g/ml), poly(dA:dT) (10 μ g/ml), poly(dG:dC) (10 μ g/ml), LM DNA (10 μ g/ml), LM (10 M.O.I.) or *E. coli* (6×10^4 CFU).

Virus Infection

Cells were infected with VSV (1 MOI), SeV (1 MOI), or HSV-1(10 MOI) for the indicated hours. Cytokine production was analyzed 24 hr later. For in vivo cytokine production studies, age- and sex-matched groups of littermate mice were intraperitoneally infected with VSV (1×10^8 pfu per mouse), SeV (1×10^3 TCID₅₀/ml per mouse), or HSV-1 (1×10^8 pfu per mouse).

Statistical Analysis

Statistical significance between groups was determined by two-tailed Student's t test and two-way ANOVA test. Differences were considered to be significant when $p < 0.05$. For mouse survival study, Kaplan-Meier survival curves were generated and analyzed for statistical significance with GraphPad Prism 4.0.

ACCESSION NUMBERS

Array data are available at Gene Expression Omnibus (<http://www.ncbi.nlm.nih.gov/geo/>) under the accession number GSE39620.

SUPPLEMENTAL INFORMATION

Supplemental Information includes Extended Experimental Procedures, seven figures and two tables and can be found with this article online at <http://dx.doi.org/10.1016/j.cell.2013.01.011>.

ACKNOWLEDGMENTS

We thank Dr. Chanrong Ni for histological processing, Dr. Jing Jin, Dr. Nan Li for helpful discussion, Dr. Zhugang Wang for providing *RigI*^{-/-} mice, and Dr. Gensheng Feng for providing *Shp2*^{fl} mice. This work was supported by the National Key Basic Research Program of China (2013CB530500 and 2012CB910202), the National Natural Science Foundation of China (81273222, 81230074, and 81123006), and the National 125 Key Project (2012ZX10002-014 and 2012AA020901). X.C. designed and supervised the research. W.C., C.H., B.X., X.H., and Q.Y. performed research. L.S., Q.W., D.L., J.W., P.Z., and Y.L. contributed new reagents/analytical tools. W.C., C.H., B.X., and X.C. analyzed data. W.C., C.H., and X.C. wrote the paper.

Received: July 27, 2012

Revised: November 2, 2012

Accepted: January 7, 2013

Published: January 31, 2013

REFERENCES

- An, H., Zhao, W., Hou, J., Zhang, Y., Xie, Y., Zheng, Y., Xu, H., Qian, C., Zhou, J., Yu, Y., et al. (2006). SHP-2 phosphatase negatively regulates the TRIF adaptor protein-dependent type I interferon and proinflammatory cytokine production. *Immunity* 25, 919–928.
- Arimoto, K., Takahashi, H., Hishiki, T., Konishi, H., Fujita, T., and Shimotohno, K. (2007). Negative regulation of the RIG-I signaling by the ubiquitin ligase RNF125. *Proc. Natl. Acad. Sci. USA* 104, 7500–7505.
- Barbalat, R., Ewald, S.E., Mouchess, M.L., and Barton, G.M. (2011). Nucleic acid recognition by the innate immune system. *Annu. Rev. Immunol.* 29, 185–214.
- Chen, G.Y., Tang, J., Zheng, P., and Liu, Y. (2009). CD24 and Siglec-10 selectively repress tissue damage-induced immune responses. *Science* 323, 1722–1725.
- Chen, G.Y., Chen, X., King, S., Cavassani, K.A., Cheng, J., Zheng, X., Cao, H., Yu, H., Qu, J., Fang, D., et al. (2011). Amelioration of sepsis by inhibiting sialidase-mediated disruption of the CD24-SiglecG interaction. *Nat. Biotechnol.* 29, 428–435.
- Chernock, R.D., Cherla, R.P., and Ganju, R.K. (2001). SHP2 and cbl participate in alpha-chemokine receptor CXCR4-mediated signaling pathways. *Blood* 97, 608–615.
- Crocker, P.R., Paulson, J.C., and Varki, A. (2007). Siglecs and their roles in the immune system. *Nat. Rev. Immunol.* 7, 255–266.
- Ding, C., Liu, Y., Wang, Y., Park, B.K., Wang, C.Y., Zheng, P., and Liu, Y. (2007). SiglecG limits the size of B1a B cell lineage by down-regulating NFkappaB activation. *PLoS ONE* 2, e997.
- Dou, H., Buetow, L., Hock, A., Sibbet, G.J., Vousden, K.H., and Huang, D.T. (2012). Structural basis for autoinhibition and phosphorylation-dependent activation of c-Cbl. *Nat. Struct. Mol. Biol.* 19, 184–192.
- Friedman, C.S., O'Donnell, M.A., Legarda-Addison, D., Ng, A., Cárdenas, W.B., Yount, J.S., Moran, T.M., Basler, C.F., Komuro, A., Horvath, C.M., et al. (2008). The tumour suppressor CYLD is a negative regulator of RIG-I-mediated antiviral response. *EMBO Rep.* 9, 930–936.
- Gack, M.U., Shin, Y.C., Joo, C.H., Urano, T., Liang, C., Sun, L., Takeuchi, O., Akira, S., Chen, Z., Inoue, S., and Jung, J.U. (2007). TRIM25 RING-finger E3 ubiquitin ligase is essential for RIG-I-mediated antiviral activity. *Nature* 446, 916–920.
- Hoffmann, A., Kerr, S., Jellusova, J., Zhang, J., Weisel, F., Wellmann, U., Winkler, T.H., Kneitz, B., Crocker, P.R., and Nitschke, L. (2007). Siglec-G is a B1 cell-inhibitory receptor that controls expansion and calcium signaling of the B1 cell population. *Nat. Immunol.* 8, 695–704.
- Hou, J., Wang, P., Lin, L., Liu, X., Ma, F., An, H., Wang, Z., and Cao, X. (2009). MicroRNA-146a feedback inhibits RIG-I-dependent Type I IFN production in macrophages by targeting TRAF6, IRAK1, and IRAK2. *J. Immunol.* 183, 2150–2158.
- Hou, F., Sun, L., Zheng, H., Skaug, B., Jiang, Q.X., and Chen, Z.J. (2011). MAVS forms functional prion-like aggregates to activate and propagate antiviral innate immune response. *Cell* 146, 448–461.
- Jiang, F., Ramanathan, A., Miller, M.T., Tang, G.Q., Gale, M., Jr., Patel, S.S., and Marcotrigiano, J. (2011). Structural basis of RNA recognition and activation by innate immune receptor RIG-I. *Nature* 479, 423–427.
- Joazeiro, C.A., Wing, S.S., Huang, H., Levenson, J.D., Hunter, T., and Liu, Y.C. (1999). The tyrosine kinase negative regulator c-Cbl as a RING-type, E2-dependent ubiquitin-protein ligase. *Science* 286, 309–312.
- Kato, H., Takahashi, K., and Fujita, T. (2011). RIG-I-like receptors: cytoplasmic sensors for non-self RNA. *Immunol. Rev.* 243, 91–98.
- Kawai, T., and Akira, S. (2010). The role of pattern-recognition receptors in innate immunity: update on Toll-like receptors. *Nat. Immunol.* 11, 373–384.
- Kawai, T., and Akira, S. (2011). Toll-like receptors and their crosstalk with other innate receptors in infection and immunity. *Immunity* 34, 637–650.

- Kowalinski, E., Lunardi, T., McCarthy, A.A., Louber, J., Brunel, J., Grigorov, B., Gerlier, D., and Cusack, S. (2011). Structural basis for the activation of innate immune pattern-recognition receptor RIG-I by viral RNA. *Cell* 147, 423–435.
- Li, N., Zhang, W., Wan, T., Zhang, J., Chen, T., Yu, Y., Wang, J., and Cao, X. (2001). Cloning and characterization of Siglec-10, a novel sialic acid binding member of the Ig superfamily, from human dendritic cells. *J. Biol. Chem.* 276, 28106–28112.
- Li, Y., Reddy, M.A., Miao, F., Shanmugam, N., Yee, J.K., Hawkins, D., Ren, B., and Natarajan, R. (2008). Role of the histone H3 lysine 4 methyltransferase, SET7/9, in the regulation of NF-kappaB-dependent inflammatory genes. Relevance to diabetes and inflammation. *J. Biol. Chem.* 283, 26771–26781.
- Liu, X., Zhan, Z., Li, D., Xu, L., Ma, F., Zhang, P., Yao, H., and Cao, X. (2011). Intracellular MHC class II molecules promote TLR-triggered innate immune responses by maintaining activation of the kinase Btk. *Nat. Immunol.* 12, 416–424.
- Loo, Y.M., and Gale, M., Jr. (2011). Immune signaling by RIG-I-like receptors. *Immunity* 34, 680–692.
- Munday, J., Kerr, S., Ni, J., Cornish, A.L., Zhang, J.Q., Nicoll, G., Floyd, H., Mattei, M.G., Moore, P., Liu, D., and Crocker, P.R. (2001). Identification, characterization and leucocyte expression of Siglec-10, a novel human sialic acid-binding receptor. *Biochem. J.* 355, 489–497.
- Negishi, H., Yanai, H., Nakajima, A., Koshiba, R., Atarashi, K., Matsuda, A., Matsuki, K., Miki, S., Doi, T., Aderem, A., et al. (2012). Cross-interference of RLR and TLR signaling pathways modulates antibacterial T cell responses. *Nat. Immunol.* 13, 659–666.
- Nielsen, P.J., Lorenz, B., Müller, A.M., Wenger, R.H., Brombacher, F., Simon, M., von der Weid, T., Langhorne, W.J., Mossmann, H., and Köhler, G. (1997). Altered erythrocytes and a leaky block in B-cell development in CD24/HSA-deficient mice. *Blood* 89, 1058–1067.
- O'Neill, L.A., and Bowie, A.G. (2011). The powerstroke and camshaft of the RIG-I antiviral RNA detection machine. *Cell* 147, 259–261.
- Oshiumi, H., Matsumoto, M., Hatakeyama, S., and Seya, T. (2009). Riplet/RNF135, a RING finger protein, ubiquitinates RIG-I to promote interferon-beta induction during the early phase of viral infection. *J. Biol. Chem.* 284, 807–817.
- Pillai, S., Netravali, I.A., Cariappa, A., and Mattoo, H. (2012). Siglecs and immune regulation. *Annu. Rev. Immunol.* 30, 357–392.
- Rehwinkel, J., and Reis e Sousa, C. (2010). RIGorous detection: exposing virus through RNA sensing. *Science* 327, 284–286.
- Schmidt, M.H., and Dikic, I. (2005). The Cbl interactome and its functions. *Nat. Rev. Mol. Cell Biol.* 6, 907–918.
- Seth, R.B., Sun, L., Ea, C.K., and Chen, Z.J. (2005). Identification and characterization of MAVS, a mitochondrial antiviral signaling protein that activates NF-kappaB and IRF 3. *Cell* 122, 669–682.
- Tanaka, Y., Tanaka, N., Saeki, Y., Tanaka, K., Murakami, M., Hirano, T., Ishii, N., and Sugamura, K. (2008). c-Cbl-dependent monoubiquitination and lysosomal degradation of gp130. *Mol. Cell. Biol.* 28, 4805–4818.
- van Kooyk, Y., and Rabinovich, G.A. (2008). Protein-glycan interactions in the control of innate and adaptive immune responses. *Nat. Immunol.* 9, 593–601.
- Vasta, G.R. (2009). Roles of galectins in infection. *Nat. Rev. Microbiol.* 7, 424–438.
- Wang, Y., Zhang, H.X., Sun, Y.P., Liu, Z.X., Liu, X.S., Wang, L., Lu, S.Y., Kong, H., Liu, Q.L., Li, X.H., et al. (2007). RIG-I^{-/-} mice develop colitis associated with downregulation of G alpha i2. *Cell Res.* 17, 858–868.
- Wang, P., Lin, C., Smith, E.R., Guo, H., Sanderson, B.W., Wu, M., Gogol, M., Alexander, T., Seidel, C., Wiedemann, L.M., et al. (2009). Global analysis of H3K4 methylation defines MLL family member targets and points to a role for MLL1-mediated H3K4 methylation in the regulation of transcriptional initiation by RNA polymerase II. *Mol. Cell. Biol.* 29, 6074–6085.
- Whitney, G., Wang, S., Chang, H., Cheng, K.Y., Lu, P., Zhou, X.D., Yang, W.P., McKinnon, M., and Longphre, M. (2001). A new siglec family member, siglec-10, is expressed in cells of the immune system and has signaling properties similar to CD33. *Eur. J. Biochem.* 268, 6083–6096.
- Xu, S., Liu, X., Bao, Y., Zhu, X., Han, C., Zhang, P., Zhang, X., Li, W., and Cao, X. (2012). Constitutive MHC class I molecules negatively regulate TLR-triggered inflammatory responses via the Fps-SHP-2 pathway. *Nat. Immunol.* 13, 551–559.
- Yang, P., An, H., Liu, X., Wen, M., Zheng, Y., Rui, Y., and Cao, X. (2010). The cytosolic nucleic acid sensor LRRFIP1 mediates the production of type I interferon via a beta-catenin-dependent pathway. *Nat. Immunol.* 11, 487–494.
- Yoneyama, M., Kikuchi, M., Natsukawa, T., Shinobu, N., Imaizumi, T., Miyagishi, M., Taira, K., Akira, S., and Fujita, T. (2004). The RNA helicase RIG-I has an essential function in double-stranded RNA-induced innate antiviral responses. *Nat. Immunol.* 5, 730–737.
- Yoneyama, M., Kikuchi, M., Matsumoto, K., Imaizumi, T., Miyagishi, M., Taira, K., Foy, E., Loo, Y.M., Gale, M., Jr., Akira, S., et al. (2005). Shared and unique functions of the DExD/H-box helicases RIG-I, MDA5, and LGP2 in antiviral innate immunity. *J. Immunol.* 175, 2851–2858.
- Zeng, W., Sun, L., Jiang, X., Chen, X., Hou, F., Adhikari, A., Xu, M., and Chen, Z.J. (2010). Reconstitution of the RIG-I pathway reveals a signaling role of unanchored polyubiquitin chains in innate immunity. *Cell* 141, 315–330.